Available online at www.sciencedirect.com
SCIENCE DIRECT®
Radiation Measurements 40 (2005) 375–379
Radiation Measurements
www.elsevier.com/locate/radmeas

Application of the ray tracing method in studying α tracks in SSNTDs

D. Nikezic[a, b], F.M.F. Ng[a], C.W.Y. Yip[a], K.N. Yu[a, *]

[a] *Department of Physics and Materials Science, City University of Hong Kong, Tat Chee Avenue, Kowloon Tong, Kowloon, Hong Kong*
[b] *Faculty of Science, University of Kragujevac, R. Domanovic 12, Serbia and MonteNegro*

Received 27 August 2004; accepted 7 February 2005

Abstract

The ray tracing method was applied to study etched tracks from α-particles in CR-39 solid-state nuclear track detectors. The transmission mode of a microscope operation was simulated. A track was considered as a set of small triangular elements, and the brightness of all elements was calculated systematically through the entire track to create the final image. Preliminary results are given for α-particle tracks in the CR-39 detector for initial energies of 4 and 4.5 MeV, and incident angles of 40 and 90°, respectively. Total reflection, as well as the slope of a surface element in the track wall, were identified as the main factors that affect the brightness of that element. At this stage, comparisons with experimental results can be made in terms of the average grey levels for the entire tracks.

Keywords: CR-39 detector; α-particles; Tracks; Ray tracing

1. Introduction

Although the optical microscope was the main tool for track observation for many years (see Nikezic and Yu, 2004), there has been relatively little investigation regarding the optical characteristics of the etched tracks. Knowledge of optical characteristics of tracks such as the average grey level can be important in automatic track measurements. Only a few papers on this topic have appeared until now and in our opinion the issue has not been fully investigated yet. McNulty et al. (1981) pointed out that conical tracks filled with some materials might be used to test the *Mie* theory of light scattering on non-spherical objects (in this case the replica of a track was taken as the conical object). They anticipated the importance of total reflection in the formation of the track image. Fews (1992) used the "mean optical density" measured by an image analysis system as an additional parameter in track studies to extend the data available for α-particles and protons. An "average brightness" of a single track was introduced to distinguish among various types of charged-particle tracks by Skvarc et al. (1992). The optical properties of a single track obtained by neutron radiography were also discussed by Assunção et al. (1994). Skvarc (1999) used a software package called POV-Ray (www.povray.com) for realistic simulation and rendering of the track images, and comparisons between simulated and measured tracks were given.

Formation of track images is a rather complicated issue, which involves (a) light scattering and reflection on the track, (b) light propagation through the optical device (microscope) used for track observation, and finally (c) track image formation in a camera or the human eye. The grey levels of the image for different parts of a track depend on the characteristics of the involved elements, and also on the

* Corresponding author. Tel.: +852 27887812; fax: +852 27887830.
E-mail address: peter.yu@cityu.edu.hk (K.N. Yu).

1350-4487/$ - see front matter © 2005 Elsevier Ltd. All rights reserved.
doi:10.1016/j.radmeas.2005.02.014

microscope settings, power of the lamp, magnification, focus used, etc.

In this paper, we will concentrate on theoretical studies of optical characteristics of tracks and limit our scope to point (a) mentioned above. We will extend our studies to points (b) and (c) in future works. We have developed our own computer program for simulation of light propagation through the tracks. The ray tracing method, based fully on geometrical optics, was applied to calculate the brightness of particular elements in the track wall. Development of our program requires a better and deeper understanding of the track image formation than that required in the application of commercially available softwares (although the images from commercial softwares may appear better to look at). However, the use of commercial softwares may not produce numerical results on the brightness of individual track elements. For example, POV-Ray (http://www.povray.org/) gives only the images. In contrast, our program will first calculate the brightness of the elements and the image is then created based on the obtained numerical data.

2. Method

2.1. Models of the track and ray propagation through the track

The track wall in three dimensions is represented by a set of points calculated by our program *test* (available on the webpage: www.cityu.edu.hk/ap/nru/test.htm) (Nikezic and Yu 2003a,b). The track wall is computed through several steps. First, the track wall in two dimensions represented by the curve μ as shown in Fig. 1 was calculated. Notations in Fig. 1 are as follows: E is the post-etching surface of the detector and OO′ is the particle path, while π, π' and π'' are planes parallel to the detector surface. The three-dimensional track wall is generated by rotating the curve μ around the particle track (OO′ axis), a cross-section of which is represented by the circles AA′ and B′BB″.

In the region closer to the track opening (see e.g., rotation of point B in Fig. 1), the track wall does not accommodate the full circle, viz., only the points on the circular arc BB′B″ are on the track wall. On getting closer to point C (the end point of the track opening), the arcs become shorter. If the distance between points is kept constant for all arcs, the number of points becomes smaller in shorter arcs. On the other hand, if the number of points is kept constant on all arcs, the distance between points becomes too small when the arc comes too close to point C. Both situations create numerical difficulties when one tries to form triangles from the points on neighbouring arcs.

In order to facilitate the simulation of light propagation through the track, some modifications of the program that create points of the three-dimensional (3-D) track have to be made. The 3-D body of the track was first cut by the planes (π, π', π'' and others) which were parallel to the detector surface (horizontal planes in panel A of Fig. 1). The intersections between these horizontal planes and the 3-D track are the horizontal semi-elliptical curves η, η', η'',... (Fig. 1). The number of points that represent the horizontal curves η was kept constant. A mesh of triangles was formed from these points to represent the track wall, which is also schematically shown in Fig. 1. The procedures of forming triangles were applied for the entire track. Some peculiarities arose when triangles were formed between the last circle η^n and the tip of the track T. In this case, all triangles have one common point T, while the other two points of the triangles are neighbouring points on η^n. To represent the track wall properly, up to 100 horizontal intersections for each track were employed.

The next step is the determination of normal lines for all triangles. For example, a triangle formed by the points $T_1(x_1, y_1, z_1)$, $T_2(x_2, y_2, z_2)$ and $T_3(x_3, y_3, z_3)$ (Fig. 1) is considered. The normal $\vec{n}$ for this triangle is given by the formula

$$\vec{n} = \begin{bmatrix} \vec{i} & \vec{j} & \vec{k} \\ x_2 - x_1 & y_2 - y_1 & z_2 - z_1 \\ x_3 - x_1 & y_3 - y_1 & z_3 - z_1 \end{bmatrix}, \tag{1}$$

where $\vec{i}, \vec{j}, \vec{k}$ are unit vectors along the axes of the coordinate system. The vector $\vec{n}$, as defined here, has a direction away from the track core towards the body of the detector, and its magnitude should also be normalized to unity.

A ray-tracing method based on geometrical optics was used in this work. The methodology is briefly outlined in this section. Here, the transmission operation mode of the microscope is considered. The light comes from the bottom as shown in panel B of Fig. 1. The light ray is represented by the vertical line which intersects at the point (x_0, y_0, z_0), which is the geometrical mean of a generated triangle, with the track wall (represented by the curve μ). The vector $\vec{p}_1$ represents the direction of the incident ray. Here, we assume that the light rays are parallel to the track. It is not appropriate to assume that the rays come from a cone for such a small object as the track. In addition, the microscope used in our experimental work has a lens between the lamp and the object, which creates a parallel beam of light. The angle between the incident light and the normal line to the surface is α, and that between the refracted light and the normal is β. The angle β is determined from the law of refraction as

$$n \sin \alpha = \sin \beta, \tag{2}$$

where n is the refractive index.

The vector $\vec{p}_2$ represents the light ray after refraction, which is determined through the following set of equations:

$$\vec{p}_1 \cdot \vec{p}_2 = \cos(\beta - \alpha), \tag{3}$$

$$\vec{n} \cdot \vec{p}_2 = -\cos \beta, \tag{4}$$

$$(\vec{p}_1 \times \vec{n}) \cdot \vec{p}_2 = 0. \tag{5}$$

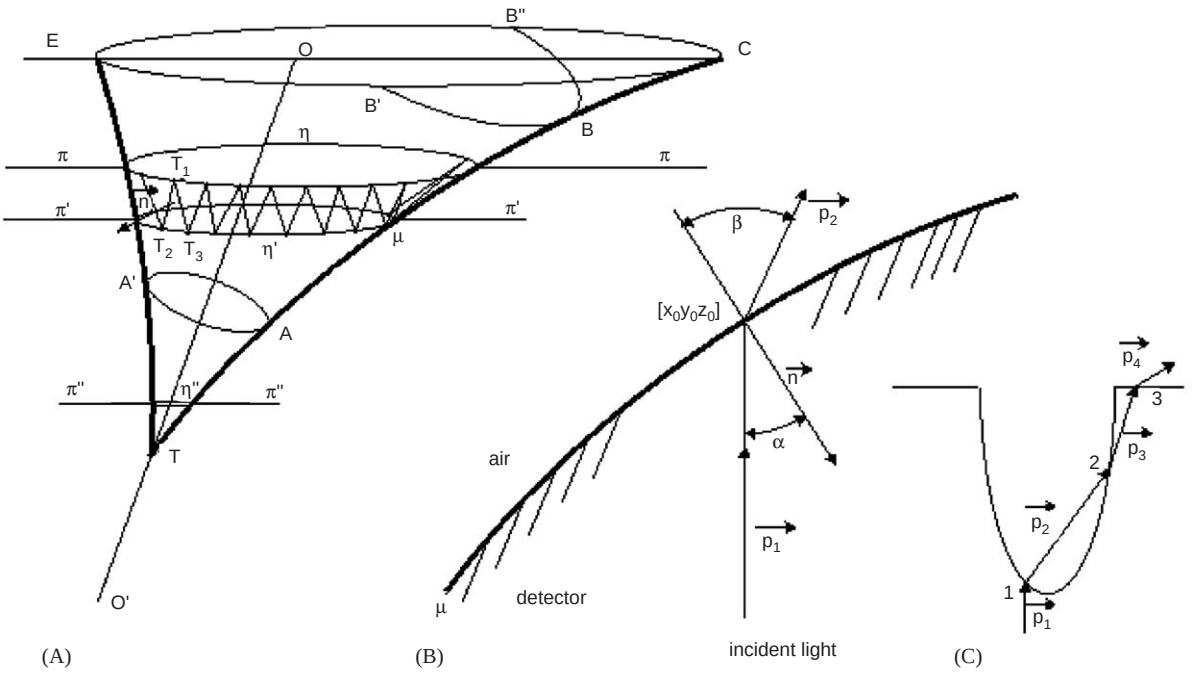

Fig. 1. Panel A: Construction of the track wall, the horizontal planes π, π' and π'', and the triangular elements on the track wall. Panel B: Refraction of a light ray at the air–detector interface. Panel C: A possible path of the light ray in the transmission operation mode of the microscope, i.e., triple refraction. Total reflection is possible at points 1 or 3. The four vectors p_i describe the path of a ray through the track.

The equations for the line describing the new light ray after refraction are as follows:

$$\frac{x - x_0}{p_{2x}} = \frac{y - y_0}{p_{2y}} = \frac{z - z_0}{p_{2z}}, \tag{6}$$

where p_{2x}, p_{2y} and p_{2z} are components of the vector $\vec{p}_2$.

The reduction of the light intensity due to the refraction on the detector–air surface was calculated by the formula given by Skvarc (1999) (as their Eq. (2)). The light ray may exit from the track through the track opening; in this case the intensity of light coming from the point (x_0, y_0, z_0) is attributed to the triangle to which that point belongs.

In some cases, the light ray may return back to the detector. This more complex case is schematically shown in panel C of Fig. 1. The new entrance point (denoted by 2) on the track wall has to be determined. Another refraction occurs at that point and a further reduction in the ray intensity has to be determined. A total of three refractions are possible for a light ray (see panel C of Fig. 1). In this case, the ray paths through the points 1, 2 and 3 are defined by four vectors, namely, $\vec{p}_1$, $\vec{p}_2$, $\vec{p}_3$ and $\vec{p}_4$, each of them being determined using formulas similar to those given above. At point 3, where the ray comes to the detector–air interface, total internal reflection is also possible. The intensity of the light ray calculated for this case is attributed to the triangle that contains point 1.

2.2. Some more details about the programs and image creation

As described above, the track wall surface was represented by a mesh of triangles. Since the track wall is a smooth surface while three points of a triangle always determine a plane, a large number of triangles have to be employed to obtain a satisfactory representation. For example, a total of 100 horizontal planes (π) each intersecting with the track wall at 100 points were used in our calculations. In this way, 200 triangles were created for one stripe between two consecutive horizontal planes.

The brightness of all triangular elements in the track wall were calculated systematically and stored in the computer memory together with the coordinates of the points. A separate program was written for graphical presentation of the track appearance. In this way, the transmission operation mode of the microscope was simulated. All the computer programs (a total of three) were written in Fortran 90. The first program (test_1.f90) generates 2-D profiles of the track wall and performs rotation of points around the main axis of the track, and also generates the points on the horizontal circles μ. The second program (track_optics.f90) simulates the light propagation through the track and calculates the relative brightness of all elements on the track wall. The mathematics and physics behind this program have been outlined in Eqs. (1)–(6). The last program (track_presentation.f90)

renders the image of the track on the computer screen based on the data generated by the second program.

Here the colour system called RGB (Red, Green, Blue) was used in image rendering. In this system, the colours are defined by hexadecimal numbers (between 0 and F). The command SETCOLORRGB(#0000FF) produces the brightest red colour, SETCOLORRGB(#00FF00) the brightest green colour, and SETCOLORRGB(#FF0000) gives the brightest blue colour. To obtain a colourless image, i.e., only black and white in different grey levels, one should mix the red, green and blue colours in equal amounts. The command SETCOLORRGB(#000000) produces a completely black object while SETCOLORRGB(#FFFFFF) creates the brightest white object. A total of 256 grey levels are available in this colour system. However, only 16 grey levels are used in this work, which are labelled with the numbers 1–16. It is noted that the results observed on the computer screen depend on the hardware used.

To calculate and present the brightness for the track elements, the following approach was used. The undamaged surface of the detector was considered completely white and the brightness was denoted as 1. In the RGB colour system, this is presented as #FFFFFF. The reduction of light intensity from particular elements was calculated using the formula given by Skvarc (1999). In this way, the relative grey levels of individual elements were obtained, which showed how much the elements were darker than the undamaged white surface. By multiplying the relative grey level with 16 and truncating the decimal part, the label of the grey colour for an element is obtained.

3. Results of ray tracing

As preliminary results, the appearance of α-particle tracks in CR-39 detectors have been determined for normal incidence and for an incident energy of 4 MeV (etching in 6.25 N aqueous NaOH for 15 h at 70 °C). The CR-39 detectors were purchased from Page Mouldings (Pershore) Limited (Worcestershire, UK). The result is shown in Fig. 2 . To calculate the track profile, the V function (which is the ratio between the track etch rate V_t and the bulk etch rate V_b) is needed. Here we used our V_t function determined previously for our detectors and etching conditions as

$$V = \frac{V_t}{V_b} = 1 + e^{-0.068R' + 1.1784} - e^{-0.6513R' + 1.1784}, \quad (7)$$

where R' is the residual range of α-particles.

This track is in the transitional conical-to-spherical phase and the opening is completely circular. There is a well-defined black ring in the track image, which originates from total internal reflection when light passes from the bottom of the detector to the track–air interface. The white spot is at the centre of the track and there is a transitional grey area between the black and white parts of the track. Although there are 16 available grey levels, the graphical capability of the computer is not enough to present the fine differences in the grey levels in the transitional area.

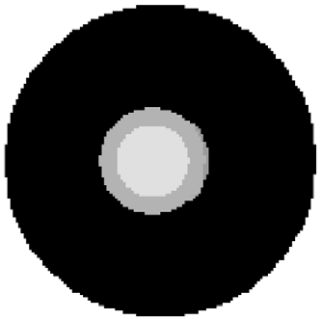

Fig. 2. The image for the track from a 4 MeV α-particle with normal incidence (after 15 h of etching at 70 °C in 6.25 N NaOH) obtained by our ray tracing and rendering programs.

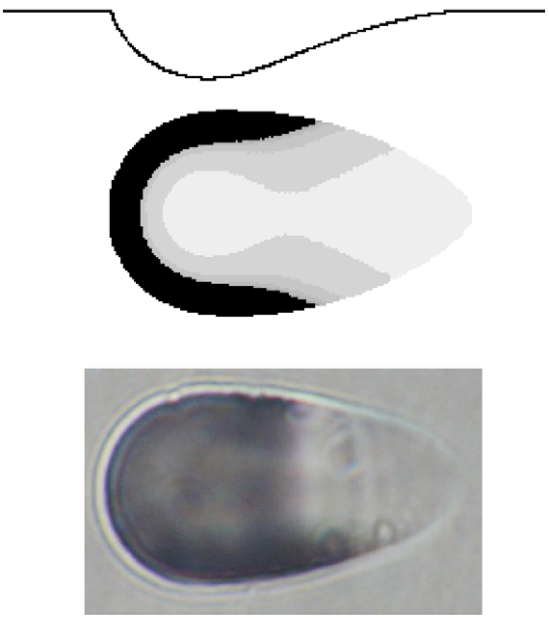

Fig. 3. Comparison between the simulated and experimentally recorded images of the tracks for an α-particle with 4.5 MeV energy and 40° incident angle (after 15 h of etching at 70 °C in 6.25 N NaOH). Top: the track profile determined by the *test* program; middle: simulated image; bottom: experimentally recorded image.

From the diameter of the white spot, d, useful information on the diameter R of the overetched part may be acquired, i.e.,

$$R \cong \frac{d}{2 \sin \theta_t}, \quad (8)$$

where θ_t is the critical angle for total reflection.

In Fig. 3, a comparison between the images of the tracks for an α-particle with 4.5 MeV energy and 40° incident angle

(etching in 6.25 N aqueous NaOH for 15 h at 70 °C) is given. The track profile (determined by the *test* program) is given on the top. The simulated image is given in the middle while the experimentally recorded image is given at the bottom. Both the simulated and the experimental images show the black rounded part due to total reflection on the left part. The slight vertical asymmetry in the experimental image is likely an artefact. Both images show a wide bright area from the centre of the track to the right end.

4. Conclusion

Simulation of light propagation through α-particle tracks in the CR-39 detector reveals that the major factors affecting the track appearances is the total internal reflection and inclination angles of elements in the track wall. Reduction of the ray intensities due to refraction has less influence on the track brightness. The ray tracing method has been shown here to be useful in the studies of nuclear tracks. It is possible to reproduce track images through computational programming. At the present stage of development of our model, we did not take into consideration the collection of light with the lenses of the microscope, propagation of light through the microscope and the image formation in the camera. Without these, comparisons with experimental results are best for the average grey levels for the entire tracks. The white spot in overetched tracks may be useful for estimation of the overetched thickness.

It is also noted here that when the track openings have size in the order of 1 μm or less, the wave properties of light might play a role in the image formation. Different wave optics effects may appear, such as light diffraction and interference.

Acknowledgements

The present research is supported by the CERG Grant CityU 102803 from the Research Grant Council of Hong Kong (City University of Hong Kong reference number 9040882).

References

Assunção, M.P.M., Pugliesi, R., De Menezes, M.O., 1994. Study of the neutron radiography characteristics for the solid state nuclear track detector Makrofol-E. Appl. Radiat. Isotop. 45, 851–855.

Fews, A.P., 1992. Flexible analysis of etched nuclear particle tracks. Nucl. Instru. Meth. B 72, 91–103.

McNulty, P.J., Palmer, S.R., Cooke, D.D., 1981. Optical properties of particle tracks in SSNTD detectors. Proceedings of the 11th International Conference on SSNTD, Bristol 7–12 September 1981, Pergamon Press, Oxford, pp. 807–813.

Nikezic, D., Yu, K.N., 2003a. Three-dimensional analytical determination of the track parameters: over-etched tracks. Radiat. Meas. 37, 39–45.

Nikezic, D., Yu, K.N., 2003b. Calculations of track parameters and plots of track openings and wall profiles in CR39 detector. Radiat. Meas. 37, 595–601.

Nikezic, D., Yu, K.N., 2004. Formation and growth of tracks in nuclear track materials. Mat. Sci. Eng. R 46, 51–123.

Skvarc, J., 1999. Optical properties of individual etched tracks. Radiat. Meas. 31, 217–222.

Skvarc, J., Ilic, R., Kodre, A., 1992. Digital evaluation of ^{6}Li(n, α) reaction product tracks in CR-39 detector. Nucl. Instru. Meth. B 71, 60–64.

www.povray.com, data accessed on 29 June 2004.